Rectangular and Circular Microstrip Disk Capacitors and Resonators

INGO WOLFF AND NORBERT KNOPPIK

Abstract—**A simple method is described to calculate the capacitances of rectangular and circular microstrip disk capacitors. From the edge capacitances of the capacitors the influence of the fringing field on the resonance frequencies of microstrip disk resonators is calculated. A theory to compute the resonance frequencies of microstrip resonators with high accuracy is presented. The resonance frequencies are calculated from a resonator model employing an effective width and length or radius, respectively, filled with a medium of a "dynamic dielectric constant." Theoretical and experimental results are compared and found to be in agreement within 1 percent.**

NOMENCLATURE

A	Amplitude factor.
C	Capacitance.
C_0	Capacitance of an air-filled disk capacitor without edge field.
c_0	Phase velocity of light in vacuum.
$C_{0,\mathrm{dyn}}$	Dynamic capacitance of a resonator without edge field.
$C_{0,\mathrm{stat}}$	Static capacitance of a capacitor without edge field.
$C_{e,\mathrm{dyn}}$	Dynamic edge capacitance.
C_{e1}, C_{e2}	Edge capacitance of the rectangular disk capacitor.
C_{dyn}	Dynamic capacitance.
E_y	y component of electric field.
E_z	z component of electric field.
f_0	Resonance frequency of new resonator model.
f_L	Resonance frequency of line resonator.
f_{meas}	Measured resonance frequency.
f_R	Resonance frequency of simple magnetic wall resonator model.
h	Substrate height.
J_n	Bessel function of nth order.
k	Wavenumber.
l	Length of rectangular capacitor/resonator.
L	Effective length of a line resonator.
l_{eff}	Effective length of a disk resonator.
l_{eq}	Effective length of a static capacitor defined by Wheeler [10].
m, n	Integer numbers.
p	"Eigenvalue," (34)–(36).
r_0	Radius of a circular disk capacitor/resonator.
r_{eff}	Effective radius of a circular disk resonator.
r, φ, z	Cylindrical coordinates.
t	Thickness of metal layer.
V	Voltage.
v_{ph1}, v_{ph2}	Phase velocities on microstrip lines of different width.
w	Width of rectangular disk capacitor/resonator/microstrip line.
W	Effective length of a line resonator.
w_{eff}	Effective width of a disk resonator.
W_{el}	Energy of electric field.
w_{eq}	Effective width of a static disk capacitor defined by Wheeler [10].
x, y, z	Cartesian coordinates.
Z	Characteristic impedance.
α_{nm}	mth zero of the derivative of the Bessel function of order n.
ϵ_0	Dielectric constant of vacuum.
ϵ_{dyn}	Dynamic dielectric constant of a disk resonator.
ϵ_{eff}	Static effective dielectric constant of a microstrip line.
ϵ_{eq}	Static effective dielectric constant of a disk capacitor.
$\epsilon_r \cdot \epsilon_0$	Dielectric constant.
λ_g	Waveguide wavelength.
δ, γ	Integer numbers.
η	Filling factor.
μ_0	Permeability of vacuum.

Manuscript received January 21, 1974; revised May 6, 1974.

I. Wolff is with the Department of Theoretical Electrotechnique, University of Duisburg, Duisburg, Germany.

N. Knoppik is with the Institute of High Frequency Techniques, the Technical University of Aachen, Aachen, Germany.

I. INTRODUCTION

MICROSTRIP disk capacitors are of interest for use in lumped element circuits [1], [2]. Farrar and Adams [3], Benedek and Silvester [4], as well as Itoh and Mittra [5] lately published numerical methods to calculate the capacitances of these capacitors. The authors have developed a very simple method to calculate the capacitances of microstrip disks, which is in very good agreement with results published by the authors mentioned above, especially for large capacitor dimensions. The results of this theory will be used to compute the resonance frequencies of rectangular and circular microstrip disk resonators. Publications present a method to calculate the resonance frequencies of circular disk resonators [6] and elliptically shaped disk resonators [7] using a magnetic wall model. A similar theory has been given for the microstrip ring resonator by the authors [8]; this theory has been used by Wu and Rosenbaum [9] to calculate the mode chart of the ring resonator. The results of the theory

given in [6] and [7] deviate from experimental results by several percents, since the edge field of the resonator and the influence of the inhomogeneous field distribution of the electric field strength on the effective dielectric constant is not considered. A theory which takes into account all these effects will be described in this paper.

II. STATIC CAPACITANCES OF DISK CAPACITORS

A rectangular microstrip disk capacitor can be considered as a degenerated microstrip line having a linewidth w and a line length l. As is well known, the characteristic impedance of the microstrip line can be calculated by a function $Z(w,h,t,\epsilon_r)$ given, e.g., by Wheeler [10] or Schneider [11]. This function $Z(w,h,t,\epsilon_r)$ renders an edge capacitance of the rectangular microstrip disk:

$$C_{e1} = \frac{1}{2}\left[\frac{1}{v_{ph1}\cdot Z(w,h,t,\epsilon_r)} - \frac{\epsilon_0\epsilon_r w}{h}\right]\cdot l$$

$$C_{e2} = \frac{1}{2}\left[\frac{1}{v_{ph2}\cdot Z(l,h,t,\epsilon_r)} - \frac{\epsilon_0\epsilon_r l}{h}\right]\cdot w. \quad (1)$$

C_{e1} is the edge capacitance at one side of length l and C_{e2} is the edge capacitance at one side of length w. The phase velocities v_{ph1} and v_{ph2} of a quasi-TEM mode on a microstrip line of width w or l, respectively, are

$$v_{ph1} = \frac{c_0\cdot Z(w,h,t,\epsilon_r)}{Z(w,h,t,\epsilon_r = 1)} \qquad v_{ph2} = \frac{c_0\cdot Z(l,h,t,\epsilon_r)}{Z(l,h,t,\epsilon_r = 1)},$$

$$c_0 = 3\cdot 10^{10}\ \text{cm/s}. \quad (2)$$

The capacitance $C(w,l,h,t,\epsilon_r)$ of the rectangular microstrip disk is then given by

$$C = \frac{\epsilon_0\epsilon_r wl}{h} + 2C_{e1} + 2C_{e2}. \quad (3)$$

From this result for the static capacitance an equivalent dielectric constant ϵ_{eq} can be defined:

$$\epsilon_{eq} = \frac{C(w,l,h,t,\epsilon_r)}{C(w,l,h,t,\epsilon_r = 1)} = \eta\cdot\epsilon_r \quad (4)$$

which is the quotient of the capacitances of a rectangular disk capacitor on a substrate material and the same disk capacitor filled with air. The equivalent dielectric constant is a function of the dimensions of the disk and the dielectric constant ϵ_r. It can be interpreted as the dielectric constant of a homogeneous medium filling the disk capacitor, so that its capacitance is equal to that given by (3); η is called the filling factor. Fig. 1 shows the capacitance $C(w,l,h,t,\epsilon_r = 1)$ normalized to $C_0 = \epsilon_0 wl/h$; Figs. 2 and 3 show the filling factor as a function of the capacitor dimensions for different values of the dielectric constant ϵ_r. Comparing the results shown in Figs. 1 and 2 to those published in [3] and [4], the deviation between C (for $\epsilon_r = 1$) from our theory and C given in [3] and [4] is negligibly small (<1 percent), provided $2h/w \leq 1$. For $2h/w \leq 2$ the deviation is on the order of 2 percent, for $2h/w \leq 4$ on the order of 20 percent, and for $2h/w \leq 10$ it

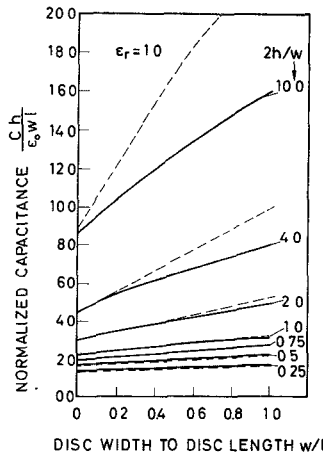

Fig. 1. The capacitance of a rectangular air-filled disk capacitor normalized to $C_0 = \epsilon_0 wl/h$ versus w/l. Parameter: $2h/w$. ——: this theory; – – –: Benedek and Silvester [4].

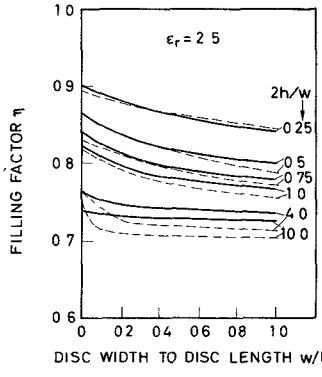

Fig. 2. Filling factor η of a rectangular disk capacitor on a dielectric sheet versus w/l for different parameters $2h/w$ and $\epsilon_r = 2.5$. ——: this theory; – – –: Benedek and Silvester [4].

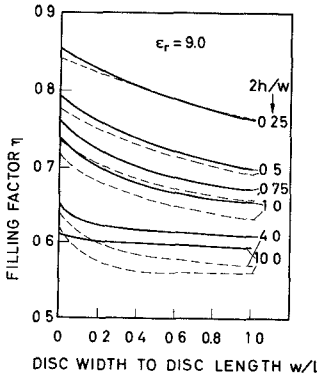

Fig. 3. Filling factor η of a rectangular disk capacitor on a dielectric sheet versus w/l for different parameters $2h/w$ and $\epsilon_r = 9$. ——: this theory; – – –: Benedek and Silvester [4].

surpasses 30 percent. Equivalent results are true for the filling factor η or the equivalent dielectric constant ϵ_{eq}, respectively. For $2h/w \leq 1$ and a dielectric constant $\epsilon_r = 2.5$ our theory and the theory described in [3] and [4] are in agreement with 1.5 percent. For $\epsilon_r = 4.2$ the deviation is about 3 percent and for $\epsilon_r = 9$ it is about 4 percent. The error of our theory increases with increasing parameter $2h/w$. For large capacitor dimensions compared to the thickness of the substrate material the total capaci-

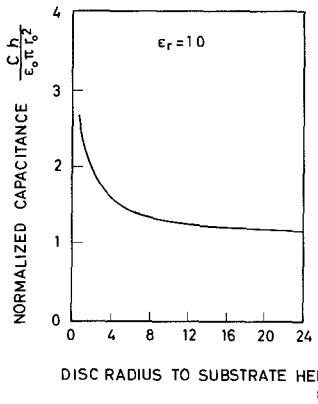

Fig. 4. The capacitance of a circular air-filled disk capacitor normalized to $C_0 = \epsilon_0 \pi r_0^2/h$ versus r_0/h.

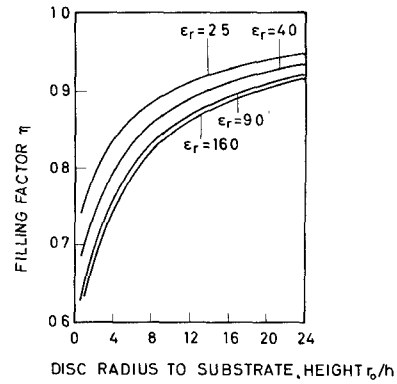

Fig. 5. Filling factor η of a circular disk capacitor on a dielectric sheet versus r_0/h for different values of ϵ_r.

tance of the rectangular disk capacitor is on the order of the main capacitance, so that the accuracy of the calculation method is high.

The capacitance of the circular disk capacitor can approximately be computed in an equally simple manner as described for the rectangular disk capacitor. The capacitance of the air-filled disk capacitor can be calculated using a formula given already by Kirchhoff [12]. This formula is a good approximation for capacitors with large radii ($r_0/h > 1$) as has been shown by Zinke [13]:

$$C = \frac{\epsilon_0 \pi r_0^2}{h} \left\{ 1 + \frac{2h}{\pi r_0} \left[\ln \left(\frac{\pi r_0}{2h} \right) + 1.7726 \right] \right\}. \quad (5)$$

Fig. 4 shows the capacitance of the air-filled circular disk capacitor normalized to the main capacitance $C_0 = \epsilon_0 \pi r_0^2/h$. Microstrip disk resonators normally have radii which fulfill the condition $r_0/h > 10$. For capacitors with such dimensions, (5) can be used to calculate the capacitance of a circular disk with an accuracy better than 1 percent.

To find an expression for the equivalent dielectric constant of the circular disk capacitor it is assumed that the edge field of the circular capacitor with large radius r_0 is similar to that of the rectangular disk capacitor.

This assumption yields for the equivalent dielectric constant ϵ_{eq}:

$$\epsilon_{eq} = \eta \cdot \epsilon_r$$

$$= \frac{\epsilon_0 \epsilon_r \pi r_0^2/h + [1/v_{ph} \cdot Z(2r_0,h,t,\epsilon_r) - 2\epsilon_0 \epsilon_r r_0/h]\pi \cdot r_0}{\epsilon_0 \pi r_0^2/h + [1/c_0 \cdot Z(2r_0,h,t,\epsilon_r = 1) - 2\epsilon_0 r_0/h]\pi \cdot r_0} \quad (6)$$

where $Z(2 \cdot r_0,h,t,\epsilon_r)$ is the characteristic impedance and v_{ph} the phase velocity of a quasi-TEM wave of a microstrip line of width $w = 2r_0$:

$$v_{ph} = \frac{c_0 \cdot Z(2r_0,h,t,\epsilon_r)}{Z(2r_0,h,t,\epsilon_r = 1)}. \quad (7)$$

Fig. 5 shows the filling factor η defined by (6) for a circular microstrip disk versus r_0/h for different values of ϵ_r. For values of $r_0/h > 10$, which normally are used for microstrip disk resonators, η is between 0.8 and 1.0. As comparisons of calculated and measured capacitances show, the accuracy of the described calculation method is, to a first approximation, the same as that for the rectangular disk capacitors.

III. THE RESONANCE FREQUENCIES OF MICROSTRIP DISK RESONATORS

A. The Circular Disk Resonator

The described method to calculate the edge capacitances of microstrip disk capacitors gives a possibility to approximate the edge fields of rectangular and circular disk resonators, as will be shown as follows.

Scientific publications present a method to calculate the resonance frequencies of circular disk resonators using a magnetic wall model of radius r_0 filled with a medium of dielectric constant ϵ_r [Fig. 6(b)] [6], [14]. Because of the small height h of the substrate materials, all fields in the resonator are of TM mode with respect to the z axis of a cylindrical coordinate system. As has been shown by Watkins [14] the resonance frequencies f_R of the resonator model with magnetic walls at $r = r_0$ can be calculated by

$$k \cdot r_0 = 2\pi f_R r_0 (\epsilon_r)^{1/2}/c_0 = \alpha_{nm} \quad (8)$$

where α_{nm} is the mth zero of the derivative of the Bessel function of order n. For $m = 1$ the zeros are

$$\alpha_{n1} = \begin{cases} 3.832, & \text{for } n = 0 \\ 1.841, & \text{for } n = 1 \\ 3.054, & \text{for } n = 2 \\ 4.201, & \text{for } n = 3. \end{cases} \quad (9)$$

Thus the lowest order mode is the TM_{110} mode, the next higher order modes are the TM_{210}, the TM_{010}, and the TM_{310} modes.

Comparing the theoretical resonance frequencies of this model with experimental results, a deviation of several percent is found (Fig. 7), since the edge field of the resonator is neglected. Fig. 7 shows the eigenvalues of the resonator model and eigenvalues calculated from measured

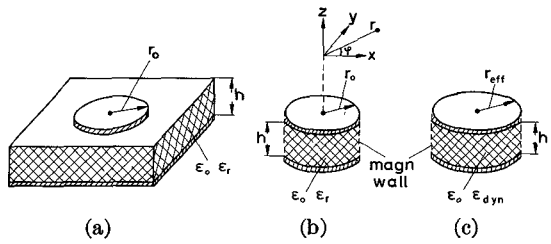

Fig. 6. (a) Microstrip circular disk resonator. (b) Simple magnetic wall model. (c) New resonator model.

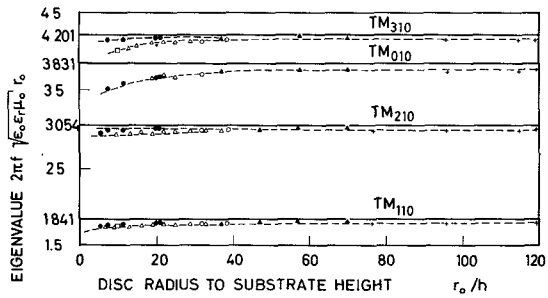

Fig. 7. Eigenvalue of the circular disk resonator calculated from the magnetic wall theory and from the measured resonance frequencies. Substrate materials: ●: Al_2O_3, h = 0.068 cm; ○: Polyguide, h = 0.078 cm; △: Polyguide, h = 0.156 cm; □: Polyguide, h = 0.312 cm; +: RT-Duroid, h = 0.0261 cm; ▲: RT-Duroid, h = 0.0531 cm.

resonance frequencies. The plots indicate the discrepancies between the magnetic wall theory and experimental data being of different magnitude for different modes of only one resonator. These discrepancies also differ for various dielectric constants even if the same mode is considered. Obviously, a more exact theory is required to describe these phenomena properly.

To accomplish this, a new resonator model is defined [Fig. 6(c)], employing an effective radius r_{eff} and a material of dynamic dielectric constant ϵ_{dyn}. The effective radius r_{eff} takes into account the electric and magnetic stray field of a resonator with homogeneous medium (e.g., $\epsilon_r = 1$). It can be calculated via the capacitance of a disk capacitor filled with air using (5):

$$r_{eff} = r_0 \left\{1 + \frac{2h}{\pi r_0}\left[\ln\left(\frac{\pi r_0}{2h}\right) + 1.7726\right]\right\}^{1/2}. \quad (10)$$

The dynamic dielectric constant ϵ_{dyn} takes into account the influence of the stray field, being partly in air and partly in the substrate material, as well as the influence of the inhomogeneous field distribution of the different modes on the effective dielectric constant. This is done in the following manner.

The electric field energy stored in the region under the disk is computed assuming the field distribution of the electric field under the disk is equal to that of the simple resonator model given by Watkins [14], Fig. 6(b):

$$W_{el} = \frac{\epsilon_0\epsilon_r}{2\delta}\cdot A^2\cdot h\cdot\pi\cdot r_0^2\cdot[J_n^2(k\cdot r_0) - J_{n-1}(k\cdot r_0) \cdot J_{n+1}(k\cdot r_0)] \quad (11)$$

with

$$\delta = \begin{cases} 1, & \text{for } n = 0 \\ 2, & \text{for } n \neq 0. \end{cases}$$

A is the amplitude of the electric field in the resonator.

Taking an arbitrarily defined voltage V at the edge of the disk resonator,

$$V = E_z(r = r_0, \varphi = 0)\cdot h = AhJ_n(kr_0) \quad (12)$$

a dynamic capacitance for the field stored under the disk may be defined by $C_{0,dyn} = 2W_{el}/V^2$:

$$C_{0,dyn} = \frac{\epsilon_0\epsilon_r\pi r_0^2}{\delta\cdot h}\left[1 - \frac{J_{n-1}(kr_0)\cdot J_{n+1}(kr_0)}{J_n^2(kr_0)}\right]. \quad (13)$$

The dynamic main capacitances of the different modes are related to the static main capacitances $C_{0,stat}$ by

$$C_{0,dyn} = \begin{cases} 1.0\cdot C_{0,stat}, & \text{for } n = 0 \\ 0.3525\cdot C_{0,stat}, & \text{for } n = 1 \\ 0.2856\cdot C_{0,stat}, & \text{for } n = 2 \\ 0.2450\cdot C_{0,stat}, & \text{for } n = 3. \end{cases} \quad (14)$$

Assuming the edge field of the resonator to have a φ-dependent field distribution as is known for the main field of the resonator model [Fig. 6(b)], a dynamic fringing capacitance can be calculated:

$$C_{e,dyn} = \frac{1}{2\pi}\int_0^{2\pi} C_{e,stat}\cdot\cos^2(n\varphi)\, d\varphi = \frac{1}{\delta}C_{e,stat}. \quad (15)$$

The total dynamic capacitance

$$C_{dyn} = C_{0,dyn} + C_{e,dyn} \quad (16)$$

yields a dynamic dielectric constant by calculating the quotient

$$\epsilon_{dyn} = \frac{C_{dyn}(\epsilon = \epsilon_0\epsilon_r)}{C_{dyn}(\epsilon = \epsilon_0)}. \quad (17)$$

ϵ_{dyn} is a function of the dimensions r_0 and h of the resonator, of the dielectric constant ϵ_r, and the field distributions of the different modes.

The resonance frequencies of the new resonator model [Fig. 6(c)] can then be computed using (10) and (17):

$$2\pi f_0 r_{eff}(\epsilon_{dyn})^{1/2}/c_0 = \alpha_{nm} \quad (18)$$

with α_{nm} given by (9).

Since the electromagnetic field in a structure with an inhomogeneous medium is known to concentrate in the region of higher dielectric constant with increasing frequency, a frequency dependence of the dynamic dielectric constant is introduced additionally. The dynamic dielectric constant is assumed to be linearly dependent on the frequency; the slope of the curve ϵ_{dyn} versus frequency is adopted to be the same as that of a microstrip line of width $2r_0$ on a substrate material with the same dielectric

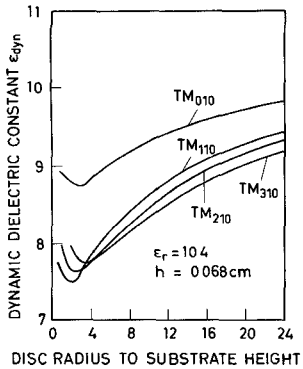

Fig. 8. The dynamic dielectric constant of a circular disk resonator for four different modes versus r_0/h. Alumina substrate (ϵ_r = 10.4), h = 0.068 cm.

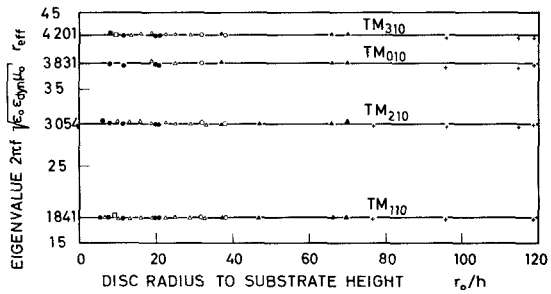

Fig. 9. Eigenvalues of the circular disk resonator calculated from (18) compared to those calculated from the measured resonance frequencies. Symbols see Fig. 7.

constant ϵ_r the resonator is built on. The dependence on frequency of the effective dielectric constant of the microstrip line is calculated via a mode-matching procedure [16].

Fig. 8 shows the dependence of the dynamic dielectric constant for a circular disk resonator on an alumina substrate material versus r_0/h, where h = 0.068 cm. It can be seen that the dynamic dielectric constant is different for the different modes. The dynamic dielectric constant reveals a minimum near values $r_0/h \approx 3$. This effect depends on the assumed dispersion characteristic. For small values of radius r_0 the resonance frequency of the resonator and thus the dynamic dielectric constant increases. The frequency dependence of the dynamic dielectric constant has been taken into account in all calculations, e.g., Fig. 9.

Fig. 9 shows the comparison between the resonance frequencies calculated by (18) and measured resonance frequencies of resonators on different substrate materials. The accuracy of calculation is better than 1 percent for all resonators and all different modes, the parameter r_0/h being in the range of $4 \leq r_0/h \leq 120$. Thus the new introduced resonator model is a good approximation to calculate the resonance frequencies of the disk resonator.

B. The Rectangular Disk Resonator

The description of the rectangular microstrip disk resonator shall distinguish between disk resonances and line resonances. On a resonator with larger width w

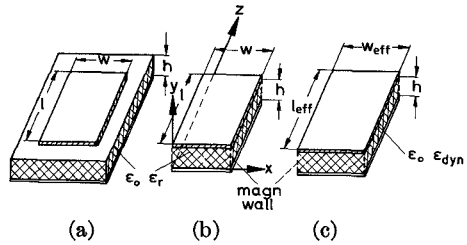

Fig. 10. (a) The rectangular disk resonator. (b) Simple magnetic wall model. (c) New resonator model.

resonances with a field dependence on the x as well as on the z coordinate can be excited. The first group of small resonators ($w < \lambda_g/2$, where λ_g is the waveguide wavelength) will be treated as line resonators, whereas the second group will be treated as disk resonators.

1) Disk Resonances: A first simple model to calculate the resonance frequencies of the disk resonances can be found, if magnetic walls are introduced at the sides of the disk with dimensions w and l as in the case of the circular disk resonator [Fig. 10(b)]. Employing this simple model, the resonance frequencies of the rectangular disk resonator (TM^y modes) can be calculated by

$$f_R = \frac{c_0}{2(\epsilon_r)^{1/2}} \left[\left(\frac{m}{w}\right)^2 + \left(\frac{n}{l}\right)^2 \right]^{1/2}, \qquad m,n = 0,1,2\cdots. \quad (19)$$

These resonance frequencies are identical to those of the electrically closed rectangular resonator.

In order to take into account the influence of the fringing field at the edges of the resonator as well as the influence of the field distributions of the different modes, a dynamic dielectric constant and an effective length and width are introduced in the same manner as described in the case of the circular resonator [Fig. 10(c)]. Assuming the field distribution of the electric field in the resonator of Fig. 10(b):

$$E_y = A \cdot \cos\left(\frac{m\pi}{w} x\right) \cos\left(\frac{n\pi}{l} z\right) \quad (20)$$

the energy stored in the electric field of the resonator is given by

$$W_{el} = \tfrac{1}{2} A^2 h \epsilon_0 \epsilon_r \frac{wl}{\delta\gamma} \quad (21)$$

with

$$\gamma = \begin{cases} 1, & \text{for } m = 0 \\ 2, & \text{for } m \neq 0 \end{cases} \quad \text{and} \quad \delta = \begin{cases} 1, & \text{for } n = 0 \\ 2, & \text{for } n \neq 0. \end{cases} \quad (22)$$

Via an arbitrarily defined voltage V at the corner of the rectangular disk ($x = 0, z = 0$) a dynamic main-field capacitance can be calculated by [see (13)]

$$C_{0,dyn} = \frac{\epsilon_0 \epsilon_r lw}{h\gamma\delta} = \frac{C_{0,stat}}{\gamma\delta} \quad (23)$$

where $C_{0,stat}$ is the static main capacitance of the disk

without considering the fringing field. A dynamic edge capacitance for each side of the resonator takes into account the influence of the fringing field, as has been described for the circular disk resonator:

$$C_{e1,\mathrm{dyn}} = \frac{1}{\delta} C_{e1,\mathrm{stat}} \qquad C_{e2,\mathrm{dyn}} = \frac{1}{\gamma} C_{e2,\mathrm{stat}}. \tag{24}$$

The dynamic main-field capacitance and the edge-field capacitances are used to calculate the total dynamic capacitance and the dynamic dielectric constant of the disk resonances as given by (17).

The resonance frequencies of the disk resonances are calculated using the resonator model of Fig. 10(c) by

$$f_0 = \frac{c_0}{2(\epsilon_{\mathrm{dyn}})^{1/2}} \left[\left(\frac{m}{w_{\mathrm{eff}}} \right)^2 + \left(\frac{n}{l_{\mathrm{eff}}} \right)^2 \right]^{1/2} \tag{25}$$

where w_{eff} and l_{eff} are the effective width and length of the resonator. w_{eff} and l_{eff} are calculated from the effective width or length w_{eq}, l_{eq}, given by Wheeler [10], taking into account the field at the corners of the disks by a phenomenological geometric method.

Fig. 11 shows the difference between the resonance frequencies of the $TM_{101}{}^{y}$ mode calculated from (25) and (19): $\Delta f = (f_0 - f_R)$ versus the parameter w/l for a resonator on Polyguide material [$\epsilon_r = 2.315$, $h = 0.156$ cm, Fig. 11(a)] and a resonator on alumina substrate material [$\epsilon_r = 10.4$, $h = 0.068$ cm, Fig. 11(b)]. Δf is always negative for resonators on Polyguide material, meaning the resonance frequencies calculated by (25) are smaller than those calculated by (19). For the resonators on alumina material Δf is negative for small values of w/l and can become positive for large values of w/l ($w/l > 0.6$). This can be explained by the dependence of the dynamic dielectric constant and the effective width on the real width w of the resonator.

2) Line Resonances: If the rectangular disk resonator has a small width w ($w < \lambda_g/2$) the fields of the resonance modes will be independent of the x coordinate. These modes shall be called line resonances. They can be classified as quasi-TEM modes with respect to the z coordinate or as $TM_{m00}{}^{y}$ and $TM_{00n}{}^{y}$ modes, if the same classification is used as for the disk resonances (see Section III-B-1)]. The resonance frequencies of the line resonances can be calculated to a first approximation by the resonance condition that the length (or width) of the disk must be a multiple of the half-wavelength $\lambda_g/2$:

$$f_L = n \frac{c_0}{2l[\epsilon_{\mathrm{eff}}(w)]^{1/2}} \tag{26}$$

and

$$f_L = m \frac{c_0}{2w[\epsilon_{\mathrm{eff}}(l)]^{1/2}} \tag{27}$$

where $\epsilon_{\mathrm{eff}}(w)$ and $\epsilon_{\mathrm{eff}}(l)$ are the effective dielectric constants of a microstrip line of width w or l, respectively, as defined by Wheeler [10] or Schneider [11]. Equations

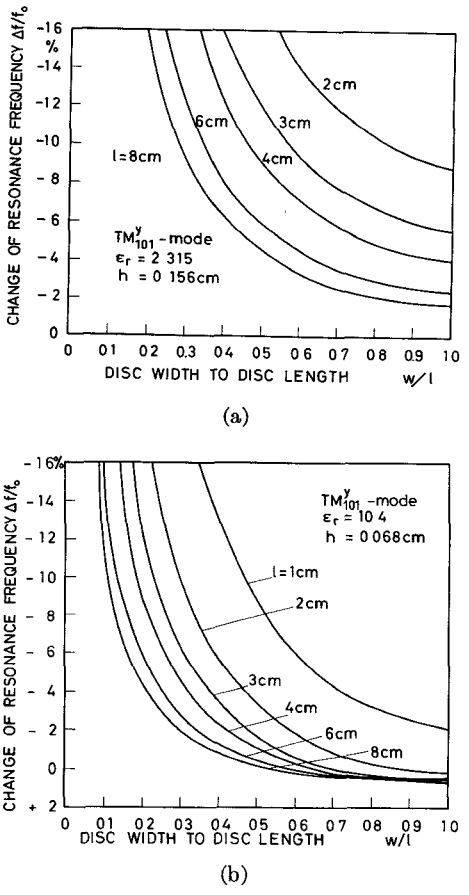

Fig. 11. Difference $\Delta f = f_0 - f_R$ (normalized to f_0) calculated from the resonance frequencies given by (25) and (19). Substrate material (a) Polyguide ($\epsilon_r = 2.315$, $h = 0.156$ cm) and (b) Al_2O_3 ($\epsilon_r = 10.4$, $h = 0.068$ cm).

(26) and (27) do not consider the influence of the fringing capacitances at the ends of the line resonator, but ϵ_{eff} includes the fringing field at the side walls of the resonator. The end capacitances can be calculated by the method given in Section II, they are, e.g., C_{e2} for the line of width w [see (1)]. The end capacitances are replaced by short pieces of open-ended lines with the same impedances as the lines of width w. If the impedance of the microstrip line of width w is written as

$$Z = \left(\frac{\mu_0}{\epsilon_0} \right)^{1/2} \cdot \frac{h}{w_{\mathrm{eq}}[\epsilon_{\mathrm{eff}}(w)]^{1/2}} \tag{28}$$

the length Δl of the open-ended lines is given by

$$\Delta l = \frac{w}{2w_{\mathrm{eq}}\epsilon_{\mathrm{dyn}}(w)} (\epsilon_{\mathrm{eff}}(l) l_{\mathrm{eq}} - \epsilon_r l) \tag{29}$$

where w_{eq} and l_{eq} are the equivalent width and length, $\epsilon_{\mathrm{eff}}(w)$ and $\epsilon_{\mathrm{eff}}(l)$ are the static effective dielectric constants, as calculated by Wheeler's [10] theory. The dynamic dielectric constant $\epsilon_{\mathrm{dyn}}(w)$ is already defined in Section III-B-1) for the disk resonances. Contrary to the case of disk resonances, in the case of line resonances, only fringing capacitances C_{e1} are considered to calculate the dynamic dielectric constant by (17), e.g., for the line resonator of width w:

$$C_{dyn} = C_{0,dyn} + 2C_{el,dyn}. \tag{30}$$

At the frequency $f = 0$ the so defined dynamic dielectric constant ϵ_{dyn} is identical to the static effective dielectric constant [10]; for higher frequencies it is the frequency dependent effective dielectric constant as known from dispersion calculations for the microstrip line, e.g., [15].

The resonance frequencies of the line resonances finally can be calculated by

$$f_0 = n \frac{c_0}{2L[\epsilon_{dyn}(w)]^{1/2}}, \qquad (TM_{00n}{}^y \text{ modes}) \tag{31}$$

for a microstrip line of width w or by

$$f_0 = m \frac{c_0}{2W[\epsilon_{dyn}(l)]^{1/2}}, \qquad (TM_{m00}{}^y \text{ modes}) \tag{32}$$

for a microstrip line of width l. The total length L and the total width W can be derived from

$$L = l + 2\Delta l \qquad W = w + 2\Delta w \tag{33}$$

where Δl is given by (29), and Δw likewise if l and w are interchanged in (29).

Fig. 12(a) shows the change $2 \cdot \Delta l$ of the length l versus w/l, resulting if the fringing capacitances at the ends of the line resonator are considered. In Fig. 12(b) the difference of the resonance frequencies: $\Delta f = f_0 - f_L$ [see (26), (27), (31), and (32)] is plotted versus w/l. The influence of the fringing capacitances at the ends of the line resonator increases if the width w of the line grows. It is large for resonators of short length l. Δf always is negative, meaning that f_0 is smaller than f_L due to the end capacitances.

3) Measurements: Several hundred disk and line resonances on substrates with different dielectric constants and different heights have been measured. Measurement has been done, exciting the resonators by small field probes with a distance above the substrate material, which could be changed continuously. Furthermore, the location of the probes above the resonators could be changed continuously in two directions. Fig. 13 shows the experimental results compared to the theoretical results. In order to achieve easy comparison between experimental and theoretical results of the different resonators (31) and (32) are rewritten in the form

$$p = 2f_{meas}[\epsilon_0 \epsilon_{dyn}(w)\mu_0]^{1/2} \cdot L = n \tag{34}$$

and

$$p = 2f_{meas}[\epsilon_0 \epsilon_{dyn}(l)\mu_0]^{1/2} \cdot W = m \tag{35}$$

where f_{meas} is the measured resonance frequency and p is an adjoint "eigenvalue." As (34) and (35) show, the eigenvalue always should be an integer number if f_{meas} is the correct resonance frequency, implying $f_{meas} = f_0$. Thus the deviation of (34) and (35) from the integer numbers n and m is a measure for the coincidence of experimental and theoretical resonance frequencies.

In the same manner an "eigenvalue" can be defined for the disk resonances:

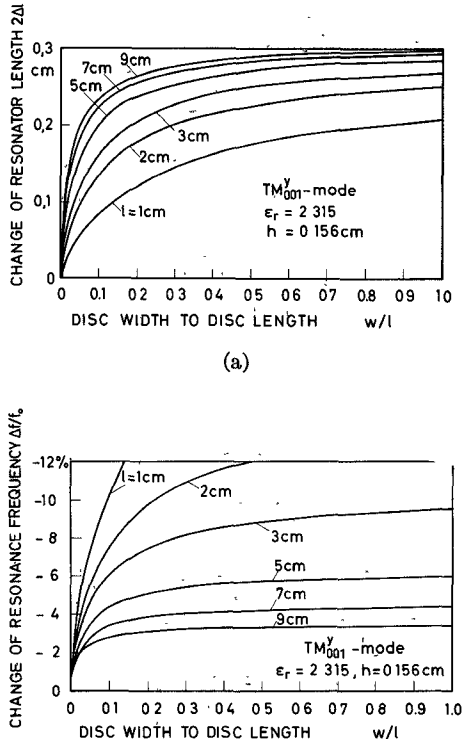

Fig. 12. Change $2 \cdot \Delta l$ of the resonator length l versus w/l, which results if the fringing capacitances at the ends of the line resonator are considered (a) and (b) the difference $\Delta f = f_0 - f_L$ (normalized to f_0) of the resonance frequencies given by (26), (27), (31), and (32).

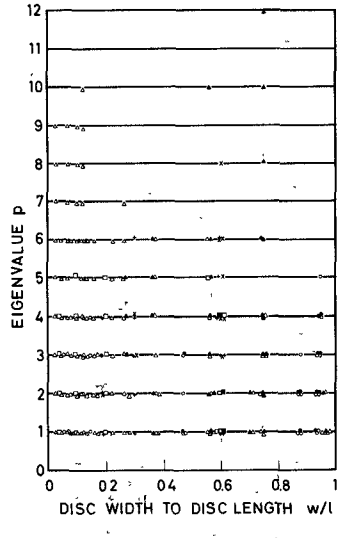

Fig. 13. Comparison between theoretical and experimental "eigenvalues" defined by (34)–(36).

$$p = \frac{2f_{meas}(\epsilon_0 \epsilon_{dyn} \mu_0)^{1/2}}{[(1/nw_{eff})^2 + (1/ml_{eff})^2]^{1/2}} \tag{36}$$

which for all resonances is an integer, if $f_{meas} = f_0$. Fig. 13 shows the measured "eigenvalues" for line resonances as well as for disk resonances. The measured resonance frequencies of the line resonances are in agreement with the theoretical results much better than 1 percent, whereas the difference between the measured and calculated resonance frequencies of the disk resonances is about

1–2 percent. This accuracy was obtained in all cases, where the resonances could be excited and detected.

SUMMARY

It has been shown that the accuracy of calculating the resonance frequencies of circular and rectangular microstrip disk resonators can be improved significantly, if a new resonator model is defined. The resonator model takes into consideration the influence of the electrical and magnetic stray field at the edges of the resonator on the effective dimensions of the resonator and the influence of the fringing field as well as the influence of the inhomogeneous field distribution of the different resonance modes on the effective dielectric constant. Using the new defined resonator models, the accuracy for calculating the resonance frequencies is about 1 percent. This result is about five to ten times better than the results of calculating methods known in the literature previously.

REFERENCES

[1] M. Caulton, B. Hershenov, S. P. Knight, and R. E. DeBrecht, "Status of lumped elements in microwave integrated circuits—Present and future," *IEEE Trans. Microwave Theory Tech. (Special Issue on Microwave Integrated Circuits)*, vol. MTT-19, pp. 588–599, July 1971.
[2] C. S. Aitchison *et al.*, "Lumped-circuit elements at microwave frequencies," *IEEE Trans. Microwave Theory Tech. (1971 Symposium Issue)*, vol. MTT-19, pp. 928–937, Dec. 1971.
[3] A. Farrar and A. T. Adams, "Matrix methods for microstrip three-dimensional problems," *IEEE Trans. Microwave Theory Tech.*, vol. MTT-20, pp. 497–504, Aug. 1972.
[4] P. Benedek and P. Silvester, "Capacitance of parallel rectangular plates separated by a dielectric sheet," *IEEE Trans. Microwave Theory Tech.*, vol. MTT-20, pp. 504–510, Aug. 1972.
[5] T. Itoh and R. Mittra, "A new method for calculating the capacitance of a circular disk for microwave integrated circuits," *IEEE Trans. Microwave Theory Tech.* (Short Papers), vol. MTT-21, pp. 431–432, June 1973.
[6] S. Mao, S. Jones, and G. D. Vendelin, "Millimeter-wave integrated circuits," *IEEE Trans. Microwave Theory Tech. (Special Issue on Microwave Integrated Circuits)*, vol. MTT-16, pp. 455–461, July 1968.
[7] J. G. Kretzschmar, "Theoretical results for the elliptic microstrip resonator," *IEEE Trans. Microwave Theory Tech.* (Short Papers), vol. MTT-20, pp. 342–343, May 1972.
[8] I. Wolff and N. Knoppik, "The microstrip ring resonator and dispersion measurements on microstrip lines," *Electron. Lett.*, vol. 7, pp. 779–781, Dec. 1971.
[9] Y. S. Wu and F. J. Rosenbaum, "Mode chart for microstrip ring resonators," *IEEE Trans. Microwave Theory Tech.* (Short Papers), vol. MTT-21, pp. 487–489, July 1973.
[10] H. A. Wheeler, "Transmission-line properties of parallel strips separated by a dielectric sheet," *IEEE Trans. Microwave Theory Tech.*, vol. MTT-13, pp. 172–185, Mar. 1965.
[11] M. V. Schneider, "Microstrip lines for microwave integrated circuits," *Bell Syst. Tech. J.*, vol. 48, pp. 1421–1444, May 1969.
[12] G. Kirchhoff, *Gesammelte Abhandlungen.* Leipzig, Germany: 1882, pp. 101–113.
[13] O. Zinke, *Widerstände, Kondensatoren, Spulen und ihre Werkstoffe.* Berlin, Germany: Springer, 1965, p. 82.
[14] J. Watkins, "Circular resonant structures in microstrip," *Electron. Lett.*, vol. 5, pp. 524–525, Oct. 16, 1969.
[15] E. J. Denlinger, "A frequency dependent solution for microstrip transmission lines," *IEEE Trans. Microwave Theory Tech.*, vol. MTT-19, pp. 30–39, Jan. 1971.
[16] H. Hofmann, "Dispersion of the ferrite-filled microstrip-line," *Arch. Elek. Übertragung.*, vol. 28, pp. 223–227, May 1974.

Hybrid Branchline Couplers—A Useful New Class of Directional Couplers

BURKHARD SCHIEK

***Abstract*—The hybrid branchline coupler consists of two transmission lines connected alternately by $\lambda/4$ shunt and series branches. The analysis of this structure leads to a class of directional couplers of which the parallel transmission-line and the de Ronde strip-slot types may be regarded as special cases. From the precise design data thus available, a number of 3-dB strip-slot couplers have been built in *C* band and *X* band with a performance close to the predicted one.**

I. INTRODUCTION

FOR the design of microwave systems with integrated circuitry the broad-band 90° 3-dB coupler is a particularly important structure and a considerable effort has been devoted to the problem of realizing such a coupler in a planar form.

Among the structures commonly used is the branchline coupler with two or three branches. This type of coupler is realizable in planar microstrip technique for a wide range of frequencies but the useful bandwidth is limited. The branchline coupler with four branches has a somewhat larger bandwidth but the impedance values of the outer branches are impractical.

Recently, the Lange coupler [1] has found wide interest but because of the necessary bonding wires the coupler is not really planar and therefore a realization at very high frequencies is difficult. Wide-band 3-dB coupling is mostly realized with the parallel-coupled transmission-line directional coupler [2]. This type of coupling is particularly suited for a triplate technique which in

Manuscript received January 21, 1974, revised March 13, 1974.
The author is with the Philips Forschungslaboratorium Hamburg GmbH, Hamburg, Germany.